Buckling and cracking of Y_2O_3 thin films at grain boundaries

Jérôme Colin,* Christophe Coupeau, Julien Durinck, and Jean Grilhé
PHYMAT-CNRS UMR 6630, Université de Poitiers, BP 30179, 86962 Futuroscope Cedex, France
(Received 12 September 2008; published 28 October 2008)

With the help of atomic force microscope, Y_2O_3 thin films deposited on GaAs(111) substrates have been evidenced to buckle and to crack at the top side of the wrinkles. This morphological evolution has been explained in the framework of Föppl–von Karman's theory of thin plates integrating two elements: the pre-existing grain and subgrain boundaries in the films leading in the early stage of buckling phenomenon to a first folding effect and in their last stage of evolution; the cracking of the buckles from the previously formed folds.

DOI: 10.1103/PhysRevB.78.153411 PACS number(s): 68.37.Ps, 62.20.mt, 46.32.+x, 61.72.Lk

For the last few years, the classical Föppl–von Karman (FvK) theory of thin plates has been popularized in the field of materials science and engineering since it has been intensively used to investigate a plethora of buckling patterns observed at the mesoscale on the surface of thin films deposited on substrates. For a wide range of materials and structures which are of fundamental technological interest, the formation of different morphologies such as circular blisters, straight-sided wrinkles, or telephone cords has been characterized within this framework.[1–8] Recently, the notion of low-angle tilt-boundary commonly used in microscopic theory of crystal plasticity has been integrated in FvK's theory of thin plates elaborated in the framework of elasticity to explain the plastic folding of buckling patterns observed on the surfaces of polycrystalline gold thin films deposited on silicon substrates.[9] The problem of ridge-cracked buckle delamination for thermal multilayers on flat and curved substrates was already studied by Faulhaber *et al.*[10] It has been found that the widths are smaller for cracked buckles on convex substrates than for uncracked buckles on flat substrates. When cracks are present, it has been also demonstrated that the critical stress for buckling is reduced to one fourth of the value obtained in the case of uncracked wrinkles.[11] Finally, it can be emphasized that the influence of the thin-film microstructure on surface damages has been recently addressed.[12] It has been shown that the Si content of Ti-Si-N films significantly reduces the appearance of buckles with cracks at their midpoint. In the present work, it is shown that pre-existing grain boundaries can initiate buckling and blister cracking. This Brief Report is organized as follows. The atomic force microscopy (AFM) observations of cracked wrinkles have been presented. In order to model this morphological evolution of the films, the equations of FvK's theory of thin plates have been solved in both cases: one wrinkle resulting from buckle splitting due to crack propagation and one wrinkle sustaining grain boundary-induced folding. A scenario describing the whole morphological evolution of the films from planar to cracked wrinkle configurations has been finally elaborated.

Y_2O_3 220-nm-thick films have been deposited by a sputtering method on GaAs(111) substrates. As evidenced by AFM (Ref. 13) in Figs. 1(a) and 1(b), the as-deposited films exhibit straight-sided buckling wrinkles characterized by a strong bending at their top side. In Figs. 1(b) and 1(c) (insert), it is observed that these folds are sometimes associated with nanometer-scale cracks partially splitting the film. According with these experimentally observed one-dimensional buckles, a straight-sided wrinkle of width $2b$ is considered along $(0y)$ axis of a thin film of thickness h [see Fig. 2(a) for axis]. Since the Young's modulus of the film ($E_f=180$ GPa) is about two times greater than the one of the substrate ($E_s=86$ GPa), the elastic effects of the substrate have been neglected and the substrate has been assimilated to a rigid support.[4,14] The initial compressive stress tensor in the planar thin film is defined as follows: $\sigma_{xx}^0=\sigma_{yy}^0=-\sigma_0$, where σ_0 is a constant. The total stress tensor in the film after buckling is thus labeled $\sigma_{ij}^{\text{tot}}=\sigma_{ij}^0+\sigma_{ij}$, where σ_{ij} is the stress variation due to the morphological change. The components of displacement variation in reference state along x, y, and z directions are, respectively, labeled u, v, and w. Since the wrinkle is assumed to be infinite along $(0y)$ axis, the displacement field (u,v,w) only depends on x variable, the v component being zero. Within the framework of nonlinear FvK's theory of thin plates, the w component of displacement satisfies[7]

$$\frac{d^4w}{dx^4}+\alpha^2\frac{d^2w}{dx^2}=0, \tag{1}$$

where α is defined as $\alpha=\sqrt{h(\sigma_0-\sigma_{xx})/D}$, with $D=E_fh^3/\{12(1-\nu_f^2)\}$ as the bending stiffness and ν_f as the Poisson's ratio of the film. (u,w) also satisfies the compatibility equations,

$$\frac{du}{dx}+\frac{1}{2}\left(\frac{dw}{dx}\right)^2=\frac{1-\nu_f^2}{E_f}\sigma_{xx}, \quad \sigma_{yy}=\nu_f\sigma_{xx}. \tag{2}$$

In the following the energies associated with the cracked and planar configurations are compared. For sake of simplicity, the case of a half wrinkle has been studied [see Fig. 2(b)]. As a consequence, the stress inside the film is assumed to be fully relaxed, which leads to $\sigma_{xx}=\sigma_0$. One thus takes $\alpha=0$ in Eq. (1). The displacement field still only depends on x, the v component being zero. The boundary conditions reduce to

$$u(0)=u(b)=w(b)=\left.\frac{dw}{dx}\right|_{x=b}=0, \quad \left.\frac{dw}{dx}\right|_{x=0^+}=-\theta, \tag{3}$$

with θ the positive angle characterizing the slope of the film near the crack edge. From Eqs. (1)–(3), one gets for $x\geq 0$

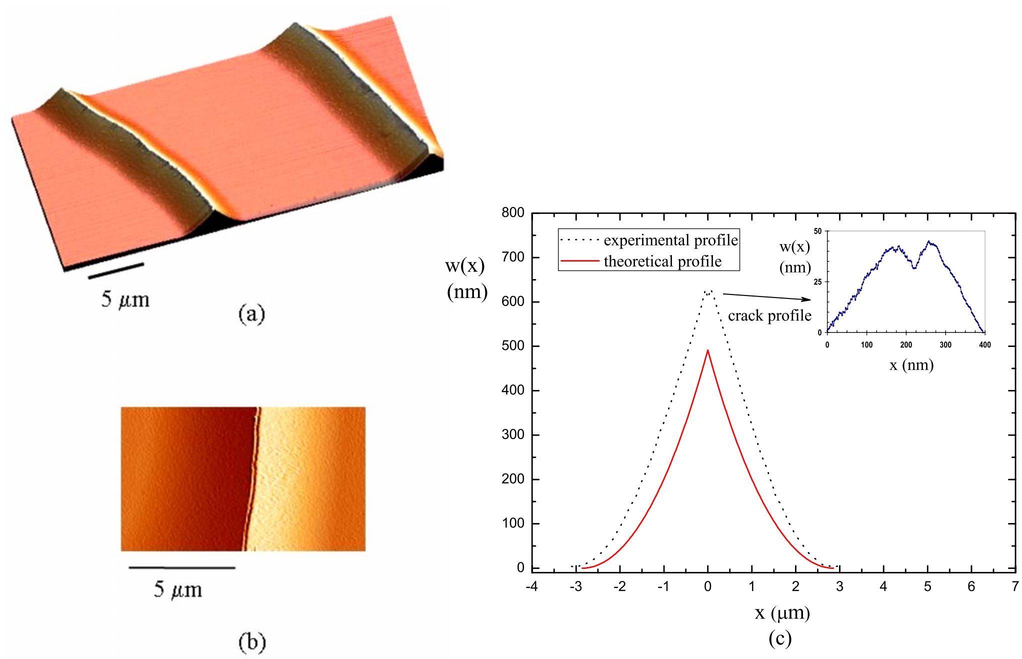

FIG. 1. (Color online) (a) Three-dimensional (3D) AFM topographical mode observation of buckles (Ref. 13). (b) Two-dimensional (2D) AFM signal error mode image of the crack at the top side of one of the wrinkles. (c) The theoretical profile of the wrinkle $[x=x+u(x),\ w(x)]$ is superimposed to the cross section of the cracked thin-film profile for an angle $\theta_{\mathrm{expt}}=20°$ and for a stress $\sigma_0=3.90$ GPa. Insert: experimental buckling profile characterized by a fold and a nanometer-scale crack at its top side.

$$u(x)=\frac{1-\nu_f^2}{E_f}\sigma_0 x-\frac{1}{2b^6}\Big\{b^6\theta^2x-2b^4\theta(2b\theta-3\lambda)x^2+\frac{2}{3}b^2(18\lambda^2-30b\lambda\theta+11b^2\theta^2)x^3-3b(6\lambda^2-7b\lambda\theta+2b^2\theta^2)x^4+\frac{9}{5}(b\theta-2\lambda)^2x^5\Big\},\tag{4}$$

$$w(x)=\frac{2\lambda-b\theta}{b^3}x^3+\frac{2b\theta-3\lambda}{b^2}x^2-\theta x+\lambda,\tag{5}$$

with $\lambda=[\theta+\sqrt{15}\sqrt{16(1-\nu_f^2)\sigma_0/E_f-\theta^2}]b/12$.

The total elastic energy variation $\Delta E_{\mathrm{el}}^{\mathrm{hw}}=\Delta E_{\mathrm{be}}+\Delta E_{\mathrm{st}}$ can be computed, with ΔE_{be} and ΔE_{st} the bending and stretching energy variations, respectively, defined with respect to planar configuration and per unit length along $(0y)$ axis;[15]

$$\Delta E_{\mathrm{be}}=\frac{E_f h^3}{24(1-\nu_f^2)}\int_{-b}^{+b}\left(\frac{d^2w}{dx^2}\right)^2dx,\tag{6}$$

$$\Delta E_{\mathrm{st}}=\frac{h}{2}\int_{-b}^{+b}\left[-2\frac{du}{dx}+\frac{E_f}{1-\nu_f^2}\left(\frac{du}{dx}\right)^2-\sigma_0\left(\frac{dw}{dx}\right)^2+\frac{E_f}{1-\nu_f^2}\left(\frac{dw}{dx}\right)^2\frac{du}{dx}+\frac{E_f}{4(1-\nu_f^2)}\left(\frac{dw}{dx}\right)^4\right]dx.\tag{7}$$

For a half wrinkle, using Eqs. (4)–(7), the total elastic energy variation with respect to the planar configuration and per unit length has been determined to be

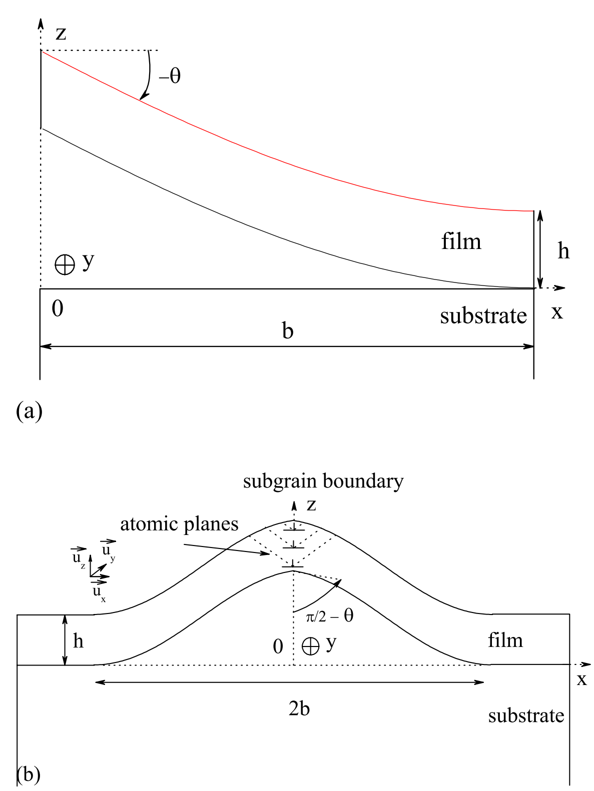

FIG. 2. (Color online) (a) A half wrinkle of thickness h and width b resulting from buckle splitting due to crack propagation. (b) A straight-sided wrinkle of width $2b$ undergoing plastic folding. A subgrain boundary made of a distribution of edge dislocations is displayed in the middle of the film which is responsible for the crystal folding.

$$\Delta E_{\mathrm{el}}^{\mathrm{hw}} = -\frac{1-\nu_f^2}{2E_f} bh\sigma_0^2 - \frac{h^3}{144(1-\nu_f^2)b} \times \{5\sqrt{15}\theta\sqrt{16(1-\nu_f^2)E_f\sigma_0 - E_f^2\theta^2} - 11E_f\theta^2 - 120\sigma_0(1-\nu_f^2)\}. \quad (8)$$

Finally, the total energy variation $\Delta E_{\mathrm{tot}}^{\mathrm{cw}}$ associated with the complete cracking and splitting of the wrinkle due to crack propagation is $\Delta E_{\mathrm{tot}}^{\mathrm{cw}} = 2\Delta E_{\mathrm{el}}^{\mathrm{hw}} + 2\Gamma h$, with Γ the toughness per unit length along $(0y)$ axis. Since the positive and constant energy term due to thin-film cracking $2\Gamma h$ is only responsible for a vertical shift in energy that will not modify the results presented in this Brief Report, it has been discarded and only the energy term redefined as $\Delta E_{\mathrm{el}}^{\mathrm{cw}} = 2\Delta E_{\mathrm{el}}^{\mathrm{hw}}$ of the cracked wrinkle has been considered in the following. In this first part, the microstructural defects of the film have not been considered. However, the thin films elaborated by physical vapor deposition contain a large number of grain and subgrain boundaries resulting in rotations and high internal stresses.[16–20] For specific grain and subgrain boundary orientations, these internal stresses may be locally relaxed by a plastic folding of the buckling structure characterized by the angle θ.

In the following, assuming that the grain and subgrain boundaries in the material may be responsible for a folding effect while buckling [see Fig. 2(b)], the energy variation associated with the buckling and folding of the film has been calculated with respect to the planar configuration. The boundary conditions are now defined by

$$u(\pm b) = w(\pm b) = \left.\frac{dw}{dx}\right|_{x=\pm b} = 0, \qquad \left.\frac{dw}{dx}\right|_{x=0^\pm} = \mp\theta \quad (9)$$

and

$$\left[\frac{dM}{dx} - \alpha^2 D\frac{dw}{dx}\right]_{|x|\neq b} = 0 \quad (10)$$

in the hypothesis where no vertical load is considered along the buckle,[21] with $M = \int_{-h/2}^{+h/2} z\sigma_{xx}^{\mathrm{tot}} dz$ as the moment. Considering Eqs. (1), (2), (9), and (10), the nonzero components of displacement field (u,w) have been found to be for $x \geq 0$

$$u(x) = \frac{1-\nu_f^2}{E_f}\left\{\sigma_0 - \alpha^2 h^2 \frac{E_f}{12(1-\nu_f^2)}\right\}x + \frac{\theta^2}{8\alpha\sin^2\alpha b}\{\sin 2\alpha(x-b) + \sin 2\alpha b - 2\alpha x\}, \quad (11)$$

$$w(x) = \frac{\theta}{\alpha}\left\{\frac{1}{\sin\alpha b} - \cot\alpha b\cos\alpha x - \sin\alpha x\right\}. \quad (12)$$

Equivalent expressions have been determined for u and w when $x<0$. The discrete set of α values is determined as a function of σ_0, θ and b, h, E_f, and ν_f parameters solving the compatibility Eq. (2),

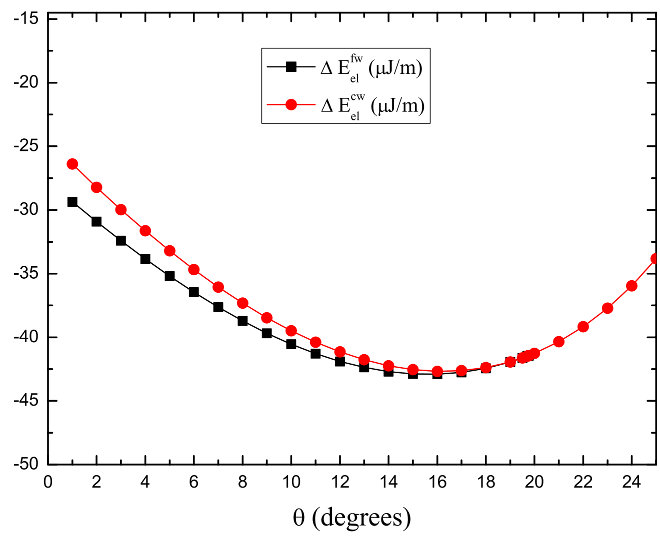

FIG. 3. (Color online) (a) $\Delta E_{\mathrm{el}}^{\mathrm{cw}}$ and $\Delta E_{\mathrm{el}}^{\mathrm{fw}}$ versus θ for $h=220$ nm, $b=2680$ nm, $E_f=180$ GPa, $\nu_f=0.29$, and $\sigma_0=3.90$ GPa.

$$\frac{2\alpha b - \sin 2\alpha b}{8\alpha b}\frac{\theta^2}{\sin^2\alpha b} = \frac{1-\nu_f^2}{E_f}\left[\sigma_0 - \alpha^2 b^2 \frac{E_f}{12(1-\nu_f^2)}\frac{h^2}{b^2}\right]. \quad (13)$$

Once the α coefficient and elastic displacements are completely determined, one gets using Eqs. (6), (7), and (11)–(13),

$$\Delta E_{\mathrm{el}}^{\mathrm{fw}} = \frac{E_f h^3\theta^2\alpha}{48(1-\nu_f^2)}\frac{2\alpha b + \sin 2\alpha b}{\sin^2\alpha b} - \frac{h}{288E_f(1-\nu_f^2)\alpha\sin^2\alpha b} \times\{\alpha b[-E_f^2\alpha^4 h^4 + 24E_f(1-\nu_f^2)\sigma_0(\alpha^2h^2+6\theta^2) - 144(1-\nu_f^2)^2\sigma_0^2] + \alpha b[E_f\alpha^2h^2 - 12\sigma_0(1-\nu_f^2)]^2\cos 2\alpha b - 72E_f(1-\nu_f^2)\sigma_0\theta^2\sin 2\alpha b\}, \quad (14)$$

with $\Delta E_{\mathrm{el}}^{\mathrm{fw}}$, the total energy variation associated with the formation of a plastically folded wrinkle. The total energy variations $\Delta E_{\mathrm{el}}^{\mathrm{cw}}$ and $\Delta E_{\mathrm{el}}^{\mathrm{fw}}$ have been plotted as a function of θ in Fig. 3 using the following parameters deduced from experimental data: $E_f=180$ GPa, $\nu_f=0.29$, $\sigma_0=3.90$ GPa, $h=220$ nm, and $b=2860$ nm. It is found that for low-angle values, i.e., for $\theta \leq 19.77°$, $\Delta E_{\mathrm{el}}^{\mathrm{fw}}$ is negative and lower than $\Delta E_{\mathrm{el}}^{\mathrm{cw}}$. For $\theta > 19.77°$, the compatibility Eq. (13) does not provide any value of α coefficient such that the plastically bent wrinkle cannot exist anymore for such high values of folding angle θ. As a consequence, the wrinkle cracking appears as a probable evolution of the structure since $\Delta E_{\mathrm{el}}^{\mathrm{cw}}$ is still negative for $\theta > 19.77°$.

The following scenario of the thin-film evolution can be then proposed. In the first stage of the buckling phenomenon, that is, for $\theta \in [0, 19.77°]$, the first energetically favorable plastic mechanism suspected to occur is the folding of the film due to grain and subgrain boundaries. For $\theta > 19.77°$, the second step of plastic deformation is the cracking of the wrinkle from the previously created fold. This scenario explains the formation of the cracked wrinkle observed in Figs. 1(a) and 1(b) with an estimated angle θ_{exp} of the order of 20°. The theoretical profile of the split wrinkle given by Eqs. (4) and (5) has been finally superimposed to the experimental one in Fig. 1(c). It can be observed that both profiles correctly match. It is suspected that the amplitude mismatch between both experimental and calculated profiles displayed in this Fig. 1(c) may be reduced by taking into consideration the elasticity of the substrate and assuming that the film is partially cracked as it has already been done in Ref. 21 using spring models.

In summary, it is found that the buckling patterns experimentally observed on the surface of Y_2O_3 thin films deposited on GaAs(111) substrates may be explained by considering two successive mechanisms of plastic deformation: the formation, in the early beginning of the buckling phenomenon, of a plastically folded buckle due to pre-existing grain and subgrain boundaries and from these precursor folds, the nucleation and propagation of cracks leading to wrinkle splitting.

*jerome.colin@univ-poitiers.fr

[1] Y. F. Liu, Y. Kagawa, and A. G. Evans, Acta Mater. **56**, 43 (2008).
[2] G. Gioia and M. Ortiz, Adv. Appl. Mech. **33**, 120 (1997).
[3] J. W. Hutchinson, M. Thouless, and E. G. Liniger, Acta Metall. Mater. **40**, 295 (1992).
[4] M. W. Moon, K. R. Lee, K. H. Oh, and J. W. Hutchinson, Acta Mater. **52**, 3151 (2004).
[5] G. Parry, A. Cimetière, C. Coupeau, J. Colin, and J. Grilhé, Phys. Rev. E **74**, 066601 (2006).
[6] E. A. Jagla, Phys. Rev. B **75**, 085405 (2007).
[7] J. W. Hutchinson and Z. Suo, Adv. Appl. Mech. **29**, 63 (1992).
[8] B. Audoly, Phys. Rev. Lett. **83**, 4124 (1999).
[9] J. Colin, C. Coupeau, and J. Grilhé, Phys. Rev. Lett. **99**, 046101 (2007).
[10] S. Faulhaber, C. Mercer, M. W. Moon, J. W. Hutchinson, and A. G. Evans, J. Mech. Phys. Solids **54**, 1004 (2006).
[11] M. D. Thouless, J. Am. Ceram. Soc. **76**, 2936 (1993).
[12] Z. J. Liu, N. Jiang, Y. G. Shen, and X. Li, Thin Solid Films **516**, 7609 (2008).
[13] I. Horcas, R. Fernàndez, J. M. Gòmez-Rodrìguez, J. Colchero, J. Gòmez-Herrero, and A. M. Baro, Rev. Sci. Instrum. **78**, 013705 (2007).
[14] B. Cotterell and Z. Chen, Int. J. Fract. **104**, 169 (2000).
[15] L. D. Landau and E. M. Lifchitz, *Theory of Elasticity*, 3rd ed. (Pergamon, New York, 1986).
[16] J. Friedel, *Dislocations* (Pergamon, London W.1, 1964).
[17] F. R. N. Nabarro, *Theory of Crystal Dislocations* (Oxford University Press, Ely House, London W.1, 1967).
[18] J. P. Hirth and J. Lothe, *Theory of Dislocations*, 2nd ed. (Wiley, New York, 1992).
[19] S. Amelinckx, *The Direct Observation of Dislocations*, Solid State Physics Suppl. 6 (Academic, New York, 1964), Vol. 1.
[20] W. T. Read and W. Shockley, Phys. Rev. **78**, 275 (1950).
[21] M. H. Zhao, F. Yang, and T. Y. Zhang, Mech. Mater. **39**, 881 (2007).